

## New Type of Multicritical Behavior in a Triangular Lattice Gas Model\*

B. Mihura† and D. P. Landau

*Department of Physics and Astronomy, University of Georgia, Athens, Georgia 30602*

(Received 27 December 1976)

A Monte Carlo study of a triangular lattice gas model appropriate to He<sup>4</sup> monolayers adsorbed on the basal plane of graphite reveals a rich variety of critical and multicritical points including a new, special type of "bicritical" point.

The theoretical interest in the critical behavior of lattice gas models has been given real, practical significance by the recent experimental studies of adsorbed gas layers on crystalline substrates.<sup>1-3</sup> The results indicate a tendency for the adsorbed atoms to lie on a regular lattice which is formed by the periodic potential of the underlying crystal. Although numerous results for surface layer adsorption exist, by far the most detailed data exist for gases adsorbed on the basal plane of graphite. The graphite surface has hexagonal symmetry and the adsorbed atoms tend to sit above hexagon centers forming, as shown in Fig. 1, a triangular lattice. Because of the large "effective area" of the gas atoms, occupation of nearest-neighbor (nn) sites on this lattice is very unfavorable, but an ordered state has been observed in which next-nearest-neighbor (nnn) sites are filled as shown in Fig. 1. An appropriate model for adsorbed gas layers is a triangular lattice gas with repulsive nn coupling. This simple model however, is equivalent to the triangular Ising lattice with antiferromagnetic nn coupling which does *not* order in zero magnetic field.<sup>4</sup> The addition of attractive nnn interactions will, however, stabilize the ordered state<sup>5</sup> shown in Fig. 1. The appropriate Hamiltonian written in terms of occupation variables  $n_i$  is

$$\mathcal{H} = V_{nn} \sum_{\text{nn pairs}} n_i n_j - V_{nnn} \sum_{\text{nnn pairs}} n_i n_k + \mu \sum_i n_i, \quad (1)$$

where  $n_i = 1$  if site  $i$  is occupied and  $n_i = 0$  otherwise.  $\mu$  is the chemical potential conjugate to the coverage  $\langle n \rangle$ . Using the simple transformation to spin variables,

$$n_i = \frac{1}{2}(1 - \sigma_i), \quad (2)$$

we readily find that Eq. (1) is equivalent to a triangular Ising model in a magnetic field:

$$\mathcal{H} = J_{nn} \sum_{\text{nn pairs}} \sigma_i \sigma_j - J_{nnn} \sum_{\text{nnn pairs}} \sigma_i \sigma_k + H \sum_i \sigma_i, \quad (3)$$

where the coverage  $\langle n \rangle$  of the lattice gas is related to the magnetization  $\langle \sigma \rangle$  of the Ising model

by Eq. (2). Campbell and Schick<sup>6</sup> studied this lattice gas model using the Bethe-Peierls-Weiss method and obtained rather unusual results. For  $\langle n \rangle = \frac{1}{2}$  (the equivalent of the Ising model in zero magnetic field) *no* ordered state was found. However, for a range of larger and smaller  $\mu$ , low-temperature ordered states appeared, separated from the liquid-gas phase by lines of first-order transitions only.

Since this problem is interesting from a purely theoretical viewpoint as well as pertinent to adsorbed gas layers, a more accurate method of study is clearly needed. We have therefore used a Monte Carlo (MC) method to study this model on  $N \times N$  rhomboid-shaped triangular lattices with periodic boundary conditions and  $12 \leq N \leq 60$ . For simplicity (and to reduce the amount of computer time required) we have studied the single ratio  $V_{nnn}/V_{nn} = 1$ . Changes in this ratio will clearly change the results in a quantitative fashion but (for a wide range of values) should not affect the qualitative features of the phase diagram. Data

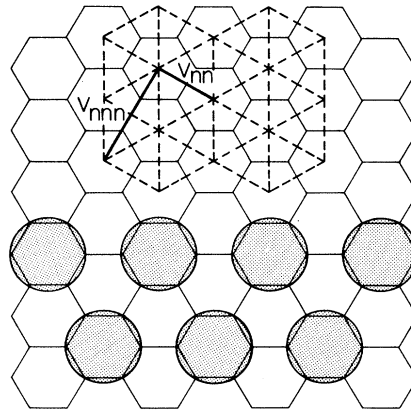


FIG. 1. Adsorbed gas atoms on a graphite substrate. The hexagons show the graphite surface structure and the shaded circles show the relative positions of the gas atoms in the ordered state. The upper portion of the diagram shows the triangular lattice formed by the possible gas atom occupation sites. The nn ( $V_{nn}$ ) and nnn ( $V_{nnn}$ ) interactions are shown by the solid lines.

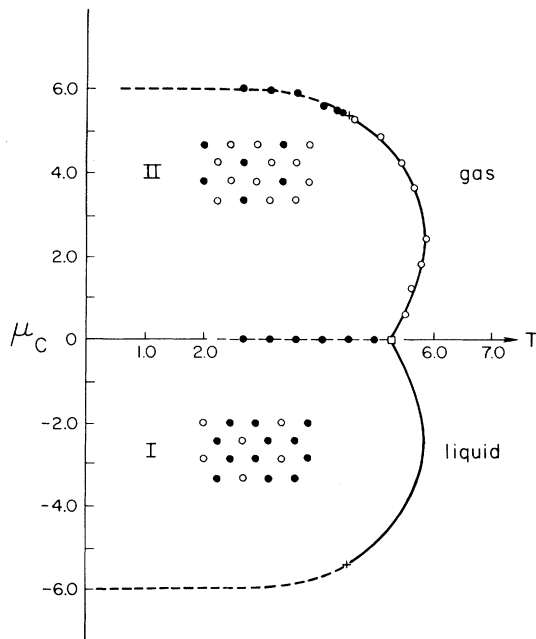


FIG. 2. Phase diagram in chemical-potential-temperature plane. The solid curves show the second-order portion of the phase boundary. The lines of first order are dashed. Actual data are only shown for the upper portion of the diagram.

were taken either at constant chemical potential or at constant temperature. Between 1000 MC step/spin and 5000 MC steps/spin were kept for calculating averages. Average values of the internal energy, coverage, and order parameter (sublattice coverage) were determined directly and the specific heat, concentration (coverage) susceptibility, and ordering susceptibility were determined from the fluctuations. The details of the method have been described elsewhere.<sup>7</sup>

From the behavior of the coverage and the specific heat we were able to trace out the phase boundaries as a function of chemical potential and temperature. The results shown in Fig. 2 indicate two different ordered states may exist (in the magnetic analog the two states are simply the time-reversed conjugates of each other). The transition between the ordered states appears to be first order all the way up to a "bicritical" (multicritical) point<sup>8</sup> (the  $\mu=0$  critical point) where both phases become simultaneously critical. As the chemical potential is increased or decreased from zero, the transition to the liquid-gas state remains second order and  $T_c$  first increases and then decreases. Eventually a tricritical point appears (for both positive and negative

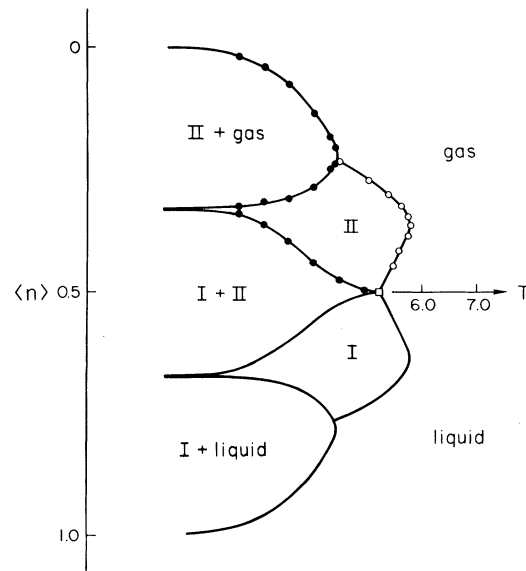


FIG. 3. Phase diagram in density-temperature plane. Data points are shown for the upper portion of the diagram (second-order points are open, first-order points are filled).

$\mu$ ) and the transition then becomes first order. These data show clearly that the Bethe-Peierls-Weiss method does not even correctly reproduce the qualitative features of the phase diagram. The corresponding variation of the critical coverage versus temperature is shown in Fig. 3. This diagram shows that both ordered phases are stable over a significant range of coverage and that the maximum critical temperature occurs, within experimental error ( $\sim \pm 0.03$ ), at coverages of  $\frac{1}{3}$  and  $\frac{2}{3}$ . Because of the existence of the mixed phases over such a wide range of  $\langle n \rangle$  and  $T$  it is clear that multiple phase transitions may be seen at constant coverage yet be missing for constant  $\mu$ . For example for  $\langle n \rangle = \text{const}$  just below  $\frac{1}{4}$  only one phase transition occurs, for a mixed phase to the liquid-gas state, whereas for  $\langle n \rangle$  just above  $\frac{1}{4}$  two transitions will be seen. This sort of behavior has apparently been observed in Kr on Grafoil<sup>9</sup> and would be expected in other gas monolayers on other substrates as well. In fact the qualitative features of the entire phase diagram should be appropriate to a wide range of adsorbed monolayers although the relative positions of the "bicritical" and tricritical points will depend on the relative strength of nn and nnn interactions. If the relative magnitude of the nnn coupling is reduced, we expect the bicritical and tricritical temperatures to be lowered. The phase diagram<sup>4</sup>

for  $V_{\text{nnn}} = 0$  supports that expectation in that the multicritical points are at  $T=0$ . From Fig. 3 we see that in systems such as rare gases on lamellar halides<sup>10</sup> where full monolayer coverage corresponds to occupation of 100% of the substrate sites the adsorption isotherms could show as many as *three* vertical steps in the process of completion of *one* monolayer.

The critical behavior of this model should be quite interesting because of the symmetry of the ordered state and the unusual nature of the phase diagram. Alexander<sup>11</sup> has suggested that the critical behavior of this model should be the same as for the three-state two-dimensional Potts model. The Potts-model exponents are, however, very close<sup>12</sup> to the Ising-model values, and in fact the critical exponents along the second-order portion of the phase boundary are consistent with either Ising or Potts values. The bicritical behavior, however, is quite different. The peak values of the specific heat for  $\mu=0$  are much smaller than for lattices of equal size and  $\mu \neq 0$ . An examination of the finite-size behavior<sup>7,13-15</sup> suggests that  $\alpha$  is negative! This conclusion is consistent with the relatively strong finite-size rounding which suggests  $\nu > 1$ . (Hyperscaling demands that  $2 - \alpha = d\nu$ ; the present data suggest that both sides of the hyperscaling equation may be greater than 2 but nonetheless equal.) A finite-size scaling analysis of the bicritical behavior of the order parameter ( $M_s$ ) indicates that  $\beta$  is much larger than either the Ising or Potts values. The finite-size scaling relation<sup>13</sup>

$$M_s N^{\beta/\nu} = f(tN^{1/\nu}), \quad (4)$$

where  $t = 1 - T/T_b$  is obeyed for  $\beta \approx 0.3 \pm 0.1$  and  $\nu$  in the range 1-1.5. A similar analysis of the ordering susceptibility suggests  $\gamma = 1.9 \pm 0.2$ . Since it appears likely that  $\alpha$  is negative, it is quite likely that the equality  $\alpha + 2\beta + \gamma = 2$  remains valid. Although it has not been possible to study the temperature dependence of the discontinuity in the magnetization across the  $\mu=0$  phase boundary closer than  $t \sim 10^{-1}$ , the behavior outside this region suggests that

$$\Delta M \propto t^{\beta_m} \quad (5)$$

with  $\beta_m = 1.5 \pm 0.4$ . This value is much larger than that obtained for the simple three-dimensional spin-flop bicritical point<sup>16</sup> ( $\beta_m \sim 0.85$ ) and, in fact, suggests that the curvature of  $\Delta M$  vs  $T$  has the *opposite* sign. It would clearly be desirable to compare the results of our study with real experi-

mental data, and adsorbed monolayers offer the only realistic possibility. Of particular interest is the "bicritical" point  $\langle n \rangle = \frac{1}{2}$ , but in many studies of real systems it has been found that the surface layer goes out of registry with the substrate and the model may no longer be applicable. The unusual multicritical behavior of this model is particularly interesting since it arises solely from the symmetry of the lattice. The role of lattice symmetry is further emphasized by the fact that the same Hamiltonian on a square lattice<sup>17</sup> does *not* produce the bicritical behavior observed on the triangular lattice.

We wish to thank Professor K. Binder, Professor M. Schick, and Professor M. Wortis for helpful discussions.

\*Research supported in part by the National Science Foundation.

<sup>†</sup>National Science Foundation Pre-college Trainee.

<sup>1</sup>M. Bretz, J. G. Dash, D. C. Hickernell, E. O. McLean, and O. E. Vilches, *Phys. Rev. A* **8**, 1589 (1973).

<sup>2</sup>J. K. Kjems, L. Passell, H. Taub, J. G. Dash, and A. D. Novaco, *Phys. Rev. B* **13**, 1446 (1976).

<sup>3</sup>J. G. Dash, *Films on Solid Surfaces* (Academic, New York, 1975).

<sup>4</sup>G. H. Wannier, *Phys. Rev.* **79**, 357 (1950). An ordered state does exist in the presence of a magnetic field and the field-induced phase transition has been studied by B. D. Metcalf, *Phys. Lett.* **45A**, 1 (1973); and by M. Schick, J. S. Walker, and M. Wortis, *Phys. Lett.* **58A**, 479 (1976). The latter line of second-order phase transitions having specific-heat exponent which is consistent with either Ising- or Potts-model values.

<sup>5</sup>B. D. Metcalf, *Phys. Lett.* **46A**, 325 (1974).

<sup>6</sup>C. E. Campbell and M. Schick, *Phys. Rev. A* **5**, 1919 (1972).

<sup>7</sup>D. P. Landau, *Phys. Rev. B* **13**, 2997 (1976).

<sup>8</sup>This "bicritical" point differs from that found in the anisotropic Heisenberg model since the effective dimensionality of the order parameter does not equal the sum of the dimensionalities associated with the two intersecting critical lines. However, until a more precise choice, dictated by a well-developed classification scheme, is available, we shall use "bicritical" because of its general descriptive nature.

<sup>9</sup>D. Butler, J. Litzinger, and G. A. Stewart, unpublished; F. A. Putnam and T. Fort, Jr., *J. Phys. Chem.* **79**, **5**, 549 (1975); A. Thomy and X. Duval, *J. Chim. Phys.* **67**, 1101 (1970).

<sup>10</sup>Y. Larher, *J. Colloid Interface Sci.* **37**, 836 (1971).

<sup>11</sup>S. Alexander, *Phys. Lett.* **54A**, 353 (1975).

<sup>12</sup>J. P. Straley and M. E. Fisher, *J. Phys. A* **6**, 1310 (1973); D. Kim and R. I. Joseph, *J. Phys. A* **8**, 891 (1975).

<sup>13</sup>M. E. Fisher, in *Critical Phenomena, Proceedings of the International School of Physics "Enrico Fermi"*,

*Course LI*, edited by M. S. Green (Academic, New York, 1971).

<sup>14</sup>D. P. Landau, *Phys. Lett.* **47A**, 41 (1974).

<sup>15</sup>E. Domany, K. K. Mon, G. V. Chester, and M. E. Fisher, *Phys. Rev. B* **12**, 5026 (1975).

<sup>16</sup>M. E. Fisher, in *Magnetism and Magnetic Materials*—

1974, edited by C. D. Graham, Jr., G. H. Lander, and J. J. Rhyne, AIP Conference Proceedings No. 24 (American Institute of Physics, New York, 1975), p. 273; J. M. Kosterlitz, D. R. Nelson, and M. E. Fisher, *Phys. Rev. B* **13**, 412 (1976).

<sup>17</sup>K. Binder and D. P. Landau, *Surf. Sci.* **61**, 577 (1976).

## Observation of the Two-Dimensional Plasmon in Silicon Inversion Layers

S. J. Allen, Jr., D. C. Tsui, and R. A. Logan

*Bell Laboratories, Murray Hill, New Jersey 07974*

(Received 18 March 1977)

The two-dimensional plasmon of an  $n$  inversion layer of (100)  $p$ -type Si is observed at a fixed wave vector as a function of electron density. The position, width, and strength of the resonance agree with existing theory at electron densities  $\geq 10^{12}/\text{cm}^2$ . At lower densities, the resonance position is below the predicted value, implying a substantial increase in the electron mass.

We have observed, in the far-infrared transmission through a silicon metal-oxide-semiconductor field-effect transistor (MOSFET), resonances which are due to plasmons in the two-dimensional (2D) electron gas that forms the inversion layer. The plasmons are coupled to the radiation field by locating a grating structure in proximity to the electron gas. At large inversion-layer electron densities,  $n_s$ , where the electron gas is metallic, the resonance position, width, and intensity agree in detail with a theory of the coupling of the plasmons and the radiation field, while at low densities,  $< 10^{12}/\text{cm}^2$ , difficulties are encountered that may be related to the anomalous electron localization often seen in these devices.

Plasma oscillations of a 2D electron gas differ in a nontrivial way from the corresponding oscillations in a 3D system. This difference stems from the fact that the restoring force for the charge-density oscillations for the 2D system is provided by the electrostatic field which remains 3D, fringing into the space on either side of the 2D sheet of charge. This has a number of important consequences that have been explored in great detail<sup>1-13</sup> from a theoretical point of view, beginning with the work of Ritchie<sup>1</sup> on thin metal foils. There are two key features. (1) The frequency of the 2D plasmon goes to zero as the wave vector goes to zero. (2) The frequency is perturbed by the shape and dielectric properties of matter in the immediate vicinity of the electron gas. In marked contrast to the extensive theoretical development, the only experiment that has directly probed the 2D plasmon is the work reported recently by Grimes and Adams<sup>14</sup> and Platz-

man and Beni<sup>15</sup> on electrons bound to a helium surface.

Our experiments were performed on an  $n$ -channel Si MOSFET with peak mobility of  $16\,000\text{ cm}^2/\text{V sec}$  at  $4.2^\circ\text{K}$ . The device was fabricated on the (100) surface of a  $p$ -Si substrate with a net acceptor concentration  $N_a - N_d = 1.1 \times 10^{15}\text{ cm}^{-3}$ . The  $1400\text{-\AA}$  dry gate oxide was grown at  $1100^\circ\text{C}$ . Fixed oxide charge  $|Q_{ss}|$  was found to be  $\leq 4 \times 10^{-10}\text{ cm}$ . Interface state density was negligible,  $< 1\%$  of the inversion-layer state density. The inversion layer was  $250\text{ }\mu\text{m} \times 250\text{ }\mu\text{m}$  with conventional source and drain contacts. The gate electrode was a semitransparent Ti film (sheet resistance  $\approx 350\text{ }\Omega/\text{sq}$ ), upon which was superimposed a grating of heavy gold metallization, with periodicity  $a = 3.52\text{ }\mu\text{m}$  (see inset of Fig. 2). The dc device characteristics were unaltered by opening the transparent regions in the gold metallization. The electron density was obtained from the gate voltage,  $V_G$ , measured from the  $77^\circ\text{K}$  conduction threshold,  $V_T$ , and the oxide capacitance per unit area,  $C_{ox}$ , by  $n_s = (C_{ox}/e)(V_G - V_T)$ . Radiation was transmitted through the inversion layer, and the fractional change in transmission  $\Delta T/T$ , caused by introducing a fixed number of inversion-layer electrons, was measured with a conventional Fourier transform spectrometer.

In the absence of the grating,  $-\Delta T/T$  measures directly the real conductivity,  $\sigma$ , of the space charge layer<sup>16</sup>

$$\text{Re}\sigma(\omega) \approx \frac{1}{2}(\Delta T/T)(Y_0 + Y_G + Y_S), \quad (1)$$

where  $Y_0$ ,  $Y_G$ , and  $Y_S$  are the wave admittances of free space, the metal gate, and the silicon sub-